is no "macrocyclic effect" comparable to the one reported for the crown ethers.[18] The internal cavities of DOTA and TETA are indeed too small to accommodate a lanthanide ion,[2,3] and the tetraaza rings simply act as frames to constrain the nitrogen atoms and the carboxylic groups into a nearly spherical arrangement.

The remarkable stability of the DOTA chelates is assigned at least partially to the favorable conformation that these compounds adopt both in the solid state and in solution. Previous studies[1,2] have shown that in crystallized NaEuDOTA, the eight donor atoms of the ligand are located at the eight vertices of a square antiprism. The repulsion energy[19] of this geometry is smaller than for any other eight-coordinate polyhedron. Furthermore, the tetraaza cycle of DOTA spans one square face of the complex and adopts its most stable and most rigid conformation, the quadrangular (3.3.3.3) structure[20] in which all CH_2 moieties are fully staggered and all nitrogen atom are pointing toward the same side of the ring. The free ligand itself probably adopts the same conformation.[20]

The stability constants of the DOTA and TETA complexes were not obtained at the same temperature, but it is obvious from a comparison of the data listed in Tables I and II that the former are considerably more stable than the latter. Several factors could account for this difference. The propylenediamine groups of the TETA cycle form six-membered rings with the metal ions. These rings are known to be sterically more crowded than the five-membered rings, a phenomenon that results in a decrease in stability as indicated by a comparison between the K_{ML} values of EuEDTA (log K_{ML} = 17.32) and of europium(III) 1,3-propanediamine-*N,N′,N″,N‴*-tetraacetate (log K_{ML} = 13.62).[17] Furthermore, in the solid state as in solution,[3,4] the TETA lanthanide chelates adopt a dodecahedral geometry. This geometry is known to exhibit a higher repulsion energy coefficient than the square antiprism, the difference being of chemical significance according to Kepert.[13]

We are now actively pursuing research that takes advantage of the high stability and the kinetic inertness of the lanthanide DOTA derivatives.

Acknowledgment. J.F.D. is grateful for support by the Fonds National de la Recherche Scientifique of Belgium. J.F.D. is Chercheur Qualifié at this institution.

Supplementary Material Available: Experimental conditions for the DOTA–oxalate competition experiments and equations plus a table of data used for calculation of K_{ML} (3 pages). Ordering information is given on any current masthead page.

---

(18) Massaux, J.; Desreux, J. F. *J. Am. Chem. Soc.* **1982**, *104*, 2967–2972.
(19) Kepert, D. L. In *Inorganic Chemistry Concepts*; Springer Verlag: Heidelberg, 1982; Vol. 6, pp 5, 152.
(20) Dale, J. *Isr. J. Chem.* **1980**, *20*, 3–11 and references cited theirin.

Contribution from the Department of Chemistry,
The University of Alberta, Edmonton, Alberta, Canada T6G 2G2

Transformation of a Terminal to a Bridging Carbonyl Ligand Accompanied by Ir–Ir Bond Cleavage: An Example of Transmission of Electronic Effects from One Metal Center to Another

Martin Cowie,* Giuseppe Vasapollo,[†] Bruce R. Sutherland, and Jimmie P. Ennett

Received December 20, 1985

The alkyne-bridged complex $[Ir_2Cl_2(CO)(\mu\text{-DMA})(DPM)_2]$ (DMA = dimethyl acetylenedicarboxylate, DPM = bis(diphenylphosphino)methane) reacts with 1 equiv of CO, PMe_3, $P(OMe)_3$, or NCMe to give one of two types of species. Reaction with CO yields the complex $[Ir_2Cl_2(CO)_2(\mu\text{-DMA})(DPM)_2]$, in which both carbonyl groups are terminally bound, one to each metal. However, reaction with L = PMe_3, $P(OMe)_3$, or NCMe yields the adducts $[Ir_2Cl_2L(\mu\text{-CO})(\mu\text{-DMA})(DPM)_2]$, in which the carbonyl group bridges the metals with no accompanying Ir–Ir bond. A rationalization of the different structures observed with the different ligands is presented. The structure of the acetonitrile adduct was determined by X-ray techniques. This species crystallizes in space group $P2_1/c$ with a = 13.060 (5) Å, b = 15.742 (2) Å, c = 30.756 (5) Å, β = 92.75 (2)°, V = 6315.9 Å^3, and Z = 4. On the basis of 5807 unique observations and 418 parameters varied, the structure converged at R = 0.051 and R_w = 0.073. The long metal–metal separation of 3.4580 (7) Å results in a geometry at the bridging carbonyl ligand that is reminiscent of sp^2 hybridization (Ir–C(O)–Ir angle of 119.4 (6)°).

Introduction

Complexes containing two or more metal centers can, in principle, give rise to reactivity patterns that differ from those displayed by single-metal-containing complexes.[1] Two fundamental characteristics that are unique to multicenter complexes, and that may therefore be important in determining reactivity differences from the mononuclear species, involve the formation of bridged-ligand bonding modes and the formation and breaking of metal–metal bonds. With the unbiquitous carbonyl ligand it seems that these two aspects are intimately connected in much of its chemistry, so that in most complexes containing bridging carbonyl groups, accompanying metal–metal bonds are also present.[2] It is only recently that examples in which bridging carbonyls *not* accompanied by metal–metal bonds have been characterized.[3-7] Although it seems clear that the presence of additional bridging groups stabilizing these species is important, it is not altogether clear what other factors may be important.

We had previously observed that the complexes $[Rh_2X_2(\mu\text{-CO})(\mu\text{-RC}_2R)(DPM)_2]$ (**1**: X = Cl, I; R = CF_3, CO_2Me; DPM = $Ph_2PCH_2PPh_2$)[5] had the unusual ketonic[8] carbonyl binding mode (structure A) but that the analogous complexes $[Ir_2Cl_2(CO)(\mu\text{-RC}_2R)(DPM)_2]$[9] (**2**) contained normal terminal CO groups (structure B). This difference is consistent with the known preference of carbonyl groups to bridge metals higher up in a triad and seems to be related, at least in part, to the increasing size of

---

[†] Present address: Centro di Studio sulle Metodologie Innovative di Sintesi Organiche del CNR, Dipartimento di Chimica, Università di Bari, 70126 Bari, Italy.

(1) Muetterties, E. L.; Rhodin, T. N.; Band, E.; Brucker, C.; Pretzer, W. R. *Chem. Rev.* **1979**, *79*, 91.
(2) Cotton, F. A.; Hunter, D. L. *Inorg. Chem.* **1974**, *13*, 2044.
(3) (a) Cotton, R.; McCormick, M. J.; Pannan, C. D. *J. Chem. Soc., Chem. Commun.* **1977**, 823. (b) Colton, R.; McCormick, M. J.; Pannan, C. D. *Aust. J. Chem.* **1978**, *31*, 1425.
(4) Brown, M. P.; Keith, A. N.; Manojlovic-Muir, Lj.; Muir, K. W.; Puddephatt, R. J.; Seddon, K. R. *Inorg. Chim. Acta* **1979**, *34*, L223.
(5) (a) Cowie, M.; Southern, T. G. *J. Organomet. Chem.* **1980**, *193*, C46. (b) Cowie, M.; Southern, T. G. *Inorg. Chem.* **1982**, *21*, 246.
(6) Kullberg, M. L., Kubiak, C. P. *Organometallics* **1984**, *3*, 632.
(7) Mague, J. T. *Inorg. Chem.* **1983**, *22*, 45.
(8) We refer to ketonic carbonyls as bridging carbonyl ligands in which there is no accompanying metal–metal bond.
(9) Sutherland, B. R.; Cowie, M. *Organometallics* **1984**, *3*, 1869.

0020-1669/86/1325-2648$01.50/0 © 1986 American Chemical Society

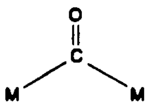

A

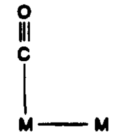

B

the metals and to the greater metal–metal bond strengths as one descends a triad.[10] The subsequent observation that the transformation of structure B in compound **2** to structure A was apparently induced upon coordination of acetonitrile caused us to question what factors might be responsible for this transformation and hence might be important in stabilizing this unusual carbonyl binding mode. Herein we report an investigation of the reactions of compound **2** with acetonitrile and related small molecules and the X-ray structure determination of the acetonitrile adduct.

Experimental Section

All solvents were dried and degassed prior to use under an atmosphere of dinitrogen. Reactions were routinely carried out by use of Schlenk conditions under a dinitrogen atmosphere. Bis(diphenylphosphino)methane (DPM), trimethylphosphine, and trimethyl phosphite were obtained from Strem Chemicals, acetonitrile was purchased from Aldrich, and hydrated iridium trichloride was obtained from Johnson Matthey. $[Ir_2Cl_2(CO)(\mu\text{-DMA})(DPM)_2]$[9] (DMA = dimethyl acetylenedicarboxylate) was prepared by the reported procedure. IR spectra were recorded on a Nicolet 7199 Fourier transform spectrometer with use of Nujol mulls on KBr plates. ^1H NMR spectra were run on either Bruker WP200 or WP400 instruments, and ^{31}P NMR spectra were obtained on either Bruker HFX-90 or WP400 instruments. The phosphorus chemical shifts are reported (upfield negative) relative to external H_3PO_4. Elemental analyses were performed within the department.

Preparation of Complexes. (a) $[Ir_2Cl_2(\mu\text{-CO})(\mu\text{-DMA})(PMe_3)(DPM)_2]$ (3). The complex $[Ir_2Cl_2(CO)(\mu\text{-DMA})(DPM)_2]$ (**2**; 205 mg, 0.147 mmol) was suspended in CH_2Cl_2 (10 mL), and 0.8 mL of a 0.187 M solution of PMe_3 in CH_2Cl_2 (0.150 mmol) was added at room temperature. The purple solid dissolved, and a yellow solution was obtained after 10 min. This solution was stirred for an additional 30 min whereupon the addition of 30 mL of diethyl ether resulted in the precipitation of a pale yellow solid, which was collected, recrystallized from THF/Et_2O, washed with ether, and dried under vacuum, giving 80–85% yields. See Table I for spectroscopic parameters for this and other compounds. Anal. Calcd for $Ir_2Cl_2P_5O_5C_{60}H_{59}$: C, 49.02; H, 4.05. Found: C, 48.91; H, 4.10.

(b) $[Ir_2Cl_2(\mu\text{-CO})(\mu\text{-DMA})(P(OMe)_3)(DPM)_2]$ (4). Compound **2** (220 mg, 0.158 mmol) was suspended in 10 mL of CH_2Cl_2 and $P(OMe)_3$ (20 μL, 0.170 mmol) was added at room temperature. The yellow solution was stirred for 60 min, and then 30 mL of diethyl ether was added, resulting in the precipitation of a yellow solid, which was collected, recrystallized from CH_2Cl_2/Et_2O, and dried under vacuum. Typical yields were about 90%. Anal. Calcd for $Ir_2Cl_2P_5O_8C_{60}H_{59}$: C, 47.47; H, 3.92. Found: C, 47.19; H, 4.20.

(c) $[Ir_2Cl_2(\mu\text{-CO})(\mu\text{-DMA})(NCCH_3)(DPM)_2]$ (5). Compound **2** (220 mg, 0.158 mmol) was suspended in CH_2Cl_2 (10 mL), and 2 mL (38.3 mmol) of CH_3CN was added. The solid dissolved after 2 h to give a purple solution. This solution was stirred for 6 days, during which time it turned yellow. A yellow solid in 93% yield was obtained by the addition of diethyl ether; recrystallization was from CH_2Cl_2/Et_2O. Anal. Calcd for $Ir_2Cl_2P_4O_5NC_{59}H_{53}$: C, 49.37; N, 0.98; H, 3.72. Found: C, 48.65; N, 0.95; H, 3.90.

(d) $[Ir_2Cl_2(CO)_2(\mu\text{-DMA})(DPM)_2]$ (6). A suspension of compound **2** (205 mg, 0.147 mmol) in 10 mL of CH_2Cl_2 was allowed to stir for 2 h under an atmosphere of carbon monoxide. A yellow solid was collected from the yellow solution by addition of diethyl ether. The formulation of the compound was confirmed by comparison of its spectroscopic properties with those of an authentic sample.[9]

X-ray Data Collection. Yellow air-stable crystals of $[Ir_2Cl_2(\mu\text{-CO})(\mu\text{-DMA})(NCCH_3)(DPM)_2]$ (**5**) were obtained by diffusion of diethyl ether into a saturated CH_2Cl_2 solution of the complex. The $2/m$ diffraction symmetry and the systematic absences unambiguously established the space group as $P2_1/c$. Accurate cell parameters were obtained from a least-squares refinement of the setting angles of 23 reflections, in the range $16.12° \leqslant 2\theta \leqslant 23.89°$, which were accurately centered on an Enraf-Nonius CAD-4 diffractometer using Mo Kα radiation. See Table II for crystal and data collection details.

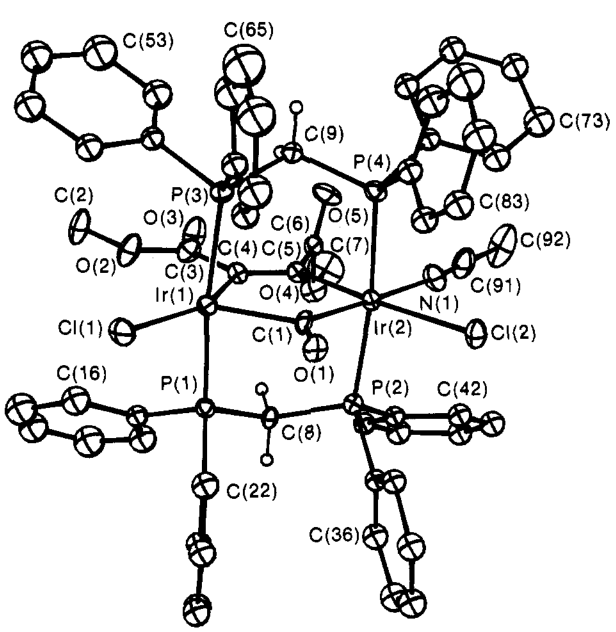

Figure 1. Perspective view of compound **5** showing the numbering scheme. Thermal ellipsoids are drawn at the 20% level.

Intensity data were collected on the CAD-4 diffractometer in the bisecting mode, employing the ω–2θ scan technique. Backgrounds were scanned for 25% of the peak width on either end of the peak scan. The intensities of three standard reflections were measured every 1 h of exposure to assess possible crystal decomposition or movement. No significant decay of these standards was noted, so no correction was applied. The data were processed in the usual way[11] by using a value of 0.04 for p. An empirical absorption correction was applied to the data by using the method of Walker and Stuart.[12]

Structure Solution and Refinement. All programs used in solution and refinement of the structure were from the Enraf-Nonius Structure Determination Package. The two independent Ir positions were deduced from a Patterson map, and all other non-hydrogen atoms were obtained from subsequent difference Fourier calculations. Atomic scattering factors[13,14] and anomalous dispersion terms[15] for Ir, Cl, and P were obtained from the usual sources. The phenyl carbon atoms were refined isotropically, and all other non-hydrogen atoms were refined anisotropically. The methyl hydrogens were not unambiguously located and so were not included in structure factor calculations; the hydrogens of the DPM groups were input in their idealized positions, with C–H distances of 0.95 Å. Each hydrogen atom was assigned an isotropic thermal parameter of 1.0 Å^2 greater than the B (or equivalent isotropic B) value of its attached carbon atom, and its position was allowed to ride on the attached carbon atom.

Although initial cycles of refinement used block-diagonal techniques, the final few cycles used full-matrix least-squares techniques, converging to the residuals given in Table II. A comparison of observed and calculated structure amplitudes showed no unusual features.

The final positional and isotropic thermal parameters are given in Table III. Additional information is presented as supplementary material.

Description of the Structure

A perspective view of $[Ir_2Cl_2(\mu\text{-CO})(\mu\text{-DMA})(NCCH_3)(DPM)_2]$ (**5**), showing the numbering scheme, is presented in Figure 1, and a view of the coordination plane approximately perpendicular to the Ir–P vectors, together with some relevant parameters, is shown in Figure 2. More complete tabulations of bond lengths and angles are given in Tables IV and V and supplementary Table VI. This structural determination confirms

---

(10) (a) Huheey, J. E. *Inorganic Chemistry: Principles of Structure and Reactivity*, 3rd ed.; Harper and Row: New York, 1983; p 601. (b) Cotton, F. A.; Wilkinson, G. *Advanced Inorganic Chemistry*, 4th ed.; Wiley: New York, 1980; p 823.

(11) Doedens, R. J.; Ibers, J. A. *Inorg. Chem.* **1967**, *6*, 204.

(12) Walker, N.; Stuart, D. *Acta Crystallogr., Sect. A: Found Crystallogr.* **1983**, *A39*, 158.

(13) Cromer, D. T.; Waber, J. t. *International Tables for X-ray Crystallography*; Kynoch: Birmingham, England, 1974; Vol. IV, Table 2.2A.

(14) Stewart, R. F.; Davidson, E. R.; Simpson, W. T. *J. Chem. Phys.* **1965**, *42*, 3175.

(15) Cromer, D. T.; Liberman, D. *J. Chem. Phys.* **1970**, *53*, 1891.

Table I. Spectral Parameters for the Compounds^a

compd	infrared, cm^{-1} ^{b,c}	NMR^d	
		$^{31}P\{^1H\}$, ppm	^1H, ppm
$[Ir_2Cl_2(CO)(\mu\text{-DMA})(DPM)_2]$ (**2**)^e	2004 (s), (1696, 1674), 1554 (w)^f	6.1 (m), −29.8 (m)	8.2–6.8 (m, 40 H), 3.98 (m, 2 H), 3.46 (m, 2 H), 2.74 (s, 3 H), 2.17 (s, 3 H)
$[Ir_2Cl_2(CO)(\mu\text{-DMA})(PMe_3)(DPM)_2]$ (**3**)	(1701, 1690), 1608, 1538 (w)^f	−5.4 (m), −27.6 (dm), −58.3 (tt) (J_{P-P} = 18.5, 1.8)^g	7.8–6.8 (m, 40 H), 4.50 (m, 2 H), 2.81 (s, 3 H), 2.25 (m, 2 H), 1.84 (s, 3 H), 1.20 (d, 9 H, J_{P-H} = 8.7)
$[Ir_2Cl_2(CO)(\mu\text{-DMA})(P(OMe)_3)(DPM)_2]$ (**4**)	(1705, 1690), 1618, 1540 (w)^f	−3.6 (m), −23.6 (m), 72.2 (t, br) (J_{P-P} = 28.3)	7.8–6.8 (m, 40 H), 4.50 (m, 2 H), 3.40 (d, 9 H, J_{P-H} = 10.1), 3.00 (s, 3 H), 2.30 (m, 2 H), 1.82 (s, 3 H)
$[Ir_2Cl_2(CO)(\mu\text{-DMA})(NCMe)(DPM)_2]$ (**5**)	(1705, 1680), 1635, 1550 (w)^f	−2.2 (m), −24.4 (m)	8.0–6.8 (m, 40 H), 4.28 (m, 2 H), 3.13 (s, 3 H), 2.35 (m, 2 H), 1.74 (s, 3 H), 1.43 (s, 3 H)^h
$[Ir_2Cl_2(CO)_2(\mu\text{-DMA})(DPM)_2]$ (**6**)^e	2023 (st), 1998 (st), (1674, 1653), 1549 (w)^f	−27.4 (m), −29.5 (m)	7.8–7.0 (m, 40 H), 4.86 (m, 2 H), 4.20 (m, 2 H), 3.24 (s, 3 H), 2.80 (s, 3 H)

^{a}Abbreviations: w, weak; st, strong; m, multiplet; dm, doublet of multiplets; tt, triple of triplets; s, singlet; t, triplet; br, broad. ^{b}Carbonyl stretches unless otherwise noted. Values in parentheses are for the DMA ligand, others are for metal carbonyls. ^{c}Bands are medium intensity unless otherwise noted. ^{d}Ambient temperature unless otherwise noted; J values in Hz. ^{e}Reference 9. $^f\nu(C{=}C)$ of dimetalated olefin. ^{g}See text for discussion of spectra. ^{h}233 K.

Table II. Summary of Crystal Data and Details of Intensity Collection

compd	$[Ir_2Cl_2(\mu\text{-CO})(\mu\text{-DMA})(NCMe)(DPM)_2]$
fw	1435.29
formula	$Ir_2Cl_2P_4O_5NC_{59}H_{53}$
space groups	$P2_1/c$
Z	4
cell params	
a, Å	13.060 (5)
b, Å	15.742 (2)
c, Å	30.756 (5)
β, deg	92.75 (2)
V, Å^3	6315.9
ρ(calcd), g/cm^3	1.509
temp, °C	22
radiatn	Mo Kα (λ = 0.71073 Å) graphite monochromated
receiving aperture, mm	3.00 + 1.00 tan θ wide by 4.0 high, 173 from cryst
takeoff angle, deg	3.0
scan speed, deg/min	variable between 0.83 and 6.67
scan width, deg	0.60 + 0.347 tan θ, in ω
2θ limits, deg	up to 50.00
μ, cm^{-1}	44.208
cryst shape	monoclinic prism with faces of the form $\{0\bar{1}1\}$, $\{100\}$, and $\{\bar{2}05\}$
range in abs cor factors^a	0.833–1.153
unique data collected	11011 ($h,k,\pm l$)
unique data used ($F_o^2 \geq 3\sigma(F_o^2)$)	5807
parameters refined	418
error in observn of unit wt	2.078
R^b	0.051
$R_w{}^c$	0.073

^{a}Empirical absorption correction using the absorption surface method of Walker and Stuart.[12] $^bR = \sum||F_o| - |F_c||/\sum|F_o|$. $^cR_w = [\sum w(|F_o| - |F_c|)^2/\sum wF_o^2]^{1/2}$.

that coordination of 1 equiv of acetonitrile has occurred and shows clearly that this has been accompanied by movement of the terminal carbonyl group to the bridging position with concomitant cleavage of the Ir–Ir bond. The geometry of the complex appears normal for a binuclear complex bridged by two essentially trans DPM groups. Orientation of the DPM ligands is such that the phenyl groups avoid the bulky dimethyl acetylenedicarboxylate ligand; consequently four of the phenyls are essentially vertical (in the view shown in Figure 1) and are aimed between the chloro ligands and the bridging carbonyl group. The coordination geometries of the two metals differ very little apart from the presence of the NCMe group on Ir(2). As a consequence, Ir(2) is pseudooctahedral with all angles about the metal approximately 90°, whereas Ir(1) is five-coordinate, although it appears almost octahedral with the site opposite C(1) being vacant. Coordination of the NCMe group at Ir(2) results in only a minor shift in the position of Cl(2) relative to Cl(1), compressing the Cl(2)–Ir(2)–C(1) angle to 98.5 (4)° compared to 114.4 (4)° for the Cl(1)–Ir(1)–C(1) angle.

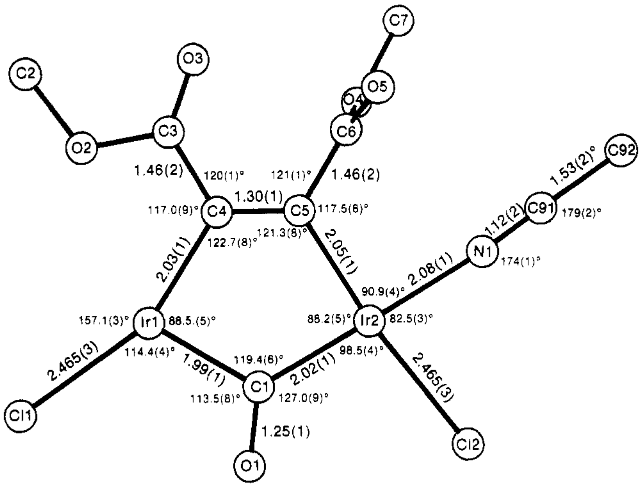

Figure 2. View of the coordination plane which is approximately perpendicular to the metal–phosphine vectors. Some relevant parameters are shown.

The Ir(1)–Ir(2) separation (3.4580 (7) Å) is very long and clearly establishes the absence of a formal Ir–Ir bond. This is substantiated by the significantly shorter intraligand P–P separations (average 3.146 (5) Å), which indicate that there is little or no mutual attraction of the two metals, as is clearly shown in Figure 1. By comparison, the Ir–Ir distance in the isoelectronic dicarbonyl species **6**, at 2.7793 (3) Å,[9] is consistent with a normal single bond. The geometry of the bridging carbonyl group in **5** is also clearly consistent with no metal—metal bond. Therefore, the Ir(1)–C(1)–Ir(2) angle of 119.4 (6)° compares well with the few other structurally characterized examples of related species[3-7] and suggests sp^2 hydridization of the CO group. In "normal" bridging carbonyls the accompanying metal–metal bonds give rise to rather acute metal–(CO)–metal angles between ca. 70 and 90°.[16] Both Ir–C(1) distances are normal and are comparable with the distances involving the bridging dimethyl acetylenedicarboxylate group in which somewhat similar bonds between Ir and sp^2 carbons are observed. The C(1)–O(1) distance (1.25 (1) Å) is certainly longer than the distances normally observed in terminal and conventional bridging CO's and is consistent with the double-bond order suggested by the sp^2 formulation. This distance is somewhat longer (although not significantly) than the

---

(16) Colton, R.; McCormick, M. J. *Coord. Chem. Rev.* **1980**, *31*, 1.

Table III. Positional and Isotropic Thermal Parameters[a]

atom	*x*	*y*	*z*	*B*, Å^2 [b]
Ir(1)	0.16009 (5)	0.20357 (4)	–0.19341 (2)	2.92 (1)*
Ir(2)	0.11690 (5)	0.08950 (4)	–0.09997 (2)	2.69 (1)*
Cl(1)	0.1054 (4)	0.3271 (3)	–0.2380 (2)	4.9 (1)*
Cl(2)	–0.0156 (4)	0.1123 (3)	–0.0467 (2)	4.7 (1)*
P(1)	0.0584 (3)	0.1019 (3)	–0.2298 (1)	2.85 (9)*
P(2)	0.0095 (3)	0.0034 (3)	–0.1440 (1)	3.0 (1)*
P(3)	0.2761 (3)	0.2827 (3)	–0.1502 (2)	3.3 (1)*
P(4)	0.2303 (3)	0.1841 (3)	–0.0645 (2)	3.4 (1)*
O(1)	0.0060 (8)	0.2359 (7)	–0.1384 (4)	4.0 (3)*
O(2)	0.3422 (9)	0.1398 (8)	–0.2345 (4)	6.1 (3)*
O(3)	0.3932 (9)	0.0236 (8)	–0.1986 (4)	6.6 (3)*
O(4)	0.2710 (9)	–0.0846 (8)	–0.1421 (4)	5.2 (3)*
O(5)	0.3771 (9)	–0.0058 (9)	–0.1018 (4)	5.7 (3)*
N(1)	0.159 (1)	–0.0091 (9)	–0.0577 (5)	4.7 (4)*
C(1)	0.079 (1)	0.186 (1)	–0.1410 (5)	3.2 (4)*
C(2)	0.426 (2)	0.130 (2)	–0.2622 (7)	7.6 (6)*
C(3)	0.334 (1)	0.081 (1)	–0.2016 (6)	4.4 (4)*
C(4)	0.248 (1)	0.1025 (9)	–0.1746 (5)	2.5 (3)*
C(5)	0.232 (1)	0.0587 (9)	–0.1398 (5)	2.6 (3)*
C(6)	0.302 (1)	–0.009 (1)	–0.1257 (5)	3.7 (4)*
C(7)	0.339 (2)	–0.160 (1)	–0.1317 (9)	9.2 (7)*
C(8)	0.048 (1)	0.001 (1)	–0.2004 (5)	2.9 (3)*
C(9)	0.325 (1)	0.227 (1)	–0.1018 (5)	3.4 (4)*
C(11)	0.111 (1)	0.066 (1)	–0.2796 (5)	3.6 (4)
C(12)	0.115 (2)	–0.022 (1)	–0.2921 (7)	6.3 (5)
C(13)	0.161 (2)	–0.043 (2)	–0.3320 (8)	8.5 (7)
C(14)	0.192 (2)	0.019 (1)	–0.3582 (8)	7.5 (6)
C(15)	0.185 (2)	0.100 (2)	–0.3497 (8)	8.1 (6)
C(16)	0.145 (2)	0.128 (1)	–0.3076 (7)	6.3 (5)
C(21)	–0.071 (1)	0.129 (1)	–0.2468 (5)	3.1 (3)
C(22)	–0.108 (1)	0.208 (1)	–0.2375 (6)	4.9 (4)
C(23)	–0.212 (1)	0.229 (1)	–0.2527 (6)	4.8 (4)
C(24)	–0.269 (1)	0.172 (1)	–0.2764 (6)	4.9 (4)
C(25)	–0.235 (2)	0.094 (1)	–0.2845 (6)	5.8 (5)
C(26)	–0.132 (1)	0.071 (1)	–0.2708 (6)	4.8 (4)
C(31)	–0.131 (1)	0.023 (1)	–0.1494 (5)	3.5 (3)
C(32)	–0.174 (1)	0.098 (1)	–0.1344 (5)	4.0 (4)
C(33)	–0.282 (1)	0.107 (1)	–0.1406 (6)	5.3 (5)
C(34)	–0.341 (2)	0.045 (1)	–0.1585 (6)	5.6 (5)
C(35)	–0.297 (2)	–0.029 (1)	–0.1725 (7)	6.1 (5)
C(36)	–0.191 (1)	–0.042 (1)	–0.1687 (6)	5.1 (4)
C(41)	0.012 (1)	–0.109 (1)	–0.1271 (5)	3.4 (3)
C(42)	–0.025 (1)	–0.123 (1)	–0.0856 (6)	4.5 (4)
C(43)	–0.026 (1	–0.207 (1)	–0.0694 (7)	5.5 (5)
C(44)	0.008 (1)	–0.272 (1)	–0.0956 (6)	5.2 (5)
C(45)	0.048 (1)	–0.256 (1)	–0.1364 (6)	5.5 (5)
C(46)	0.050 (1)	–0.172 (1)	–0.1526 (6)	4.1 (4)
C(51)	0.391 (1)	0.310 (1)	–0.1764 (5)	3.7 (4)
C(52)	0.483 (2)	0.275 (1)	–0.1648 (7)	6.3 (5)
C(53)	0.572 (2)	0.304 (2)	–0.1871 (8)	8.7 (7)
C(54)	0.564 (2)	0.365 (1)	–0.2214 (7)	7.2 (6)
C(55)	0.467 (2)	0.395 (1)	–0.2335 (7)	6.5 (5)
C(56)	0.381 (1)	0.366 (1)	–0.2111 (6)	5.1 (4)
C(61)	0.240 (1)	0.385 (1)	–0.1298 (6)	4.3 (4)
C(62)	0.140 (1)	0.415 (1)	–0.1337 (6)	4.5 (4)
C(63)	0.117 (2)	0.494 (1)	–0.1183 (7)	6.6 (5)
C(64)	0.188 (2)	0.541 (2)	–0.0980 (8)	8.6 (7)
C(65)	0.286 (2)	0.514 (2)	–0.0939 (9)	10.3 (8)
C(66)	0.315 (2)	0.434 (1)	–0.1107 (8)	7.6 (6)
C(71)	0.304 (1)	0.137 (1)	–0.0191 (5)	3.5 (4)
C(72)	0.247 (2)	0.104 (1)	0.0154 (6)	5.8 (5)
C(73)	0.296 (2)	0.066 (1)	0.0520 (8)	7.0 (6)
C(74)	0.406 (1)	0.061 (1)	0.0546 (7)	5.9 (5)
C(75)	0.463 (2)	0.090 (1)	0.0216 (6)	5.5 (5)
C(76)	0.412 (1)	0.128 (1)	–0.0168 (6)	4.7 (4)
C(81)	0.180 (1)	0.279 (1)	–0.0377 (6)	4.2 (4)
C(82)	0.082 (1)	0.307 (1)	–0.0419 (6)	4.4 (4)
C(83)	0.044 (1)	0.373 (1)	–0.0191 (6)	5.1 (4)
C(84)	0.104 (2)	0.414 (1)	0.0087 (7)	6.6 (5)
C(85)	0.203 (2)	0.391 (2)	0.0162 (8)	8.3 (7)
C(86)	0.243 (2)	0.320 (1)	–0.0063 (7)	6.7 (6)
C(91)	0.190 (1)	–0.062 (1)	–0.0363 (7)	6.0 (5)*
C(92)	0.229 (2)	–0.134 (1)	–0.0068 (8)	10.2 (7)*

[a] Numbers in parentheses are estimated standard deviations in the least significant digits. [b] Asterisks indicate the equivalent isotopic thermal parameters for atoms that were refined anisotropically.

Table IV. Selected Distances (Å) for Compound **5**[a]

	(a) Bond Distances		
Ir(1)–Cl(1)	2.465 (3)	P(3)–C(51)	1.79 (1)
Ir(1)–P(1)	2.331 (3)	P(3)–C(61)	1.80 (1)
Ir(1)–P(3)	2.328 (3)	P(4)–C(9)	1.86 (1)
Ir(1)–C(1)	1.990 (11)	P(4)–C(71)	1.82 (1)
Ir(1)–C(4)	2.033 (10)	P(4)–C(81)	1.84 (1)
Ir(2)–Cl(2)	2.465 (3)	O(1)–C(1)	1.25 (1)
Ir(2)–P(2)	2.337 (3)	O(2)–C(2)	1.43 (2)
Ir(2)–P(4)	2.334 (3)	O(2)–C(3)	1.38 (2)
Ir(2)–N(1)	2.082 (11)	O(3)–C(3)	1.20 (1)
Ir(2)–C(1)	2.015 (12)	O(4)–C(6)	1.34 (1)
Ir(2)–C(5)	2.047 (10)	O(4)–C(7)	1.51 (2)
P(1)–C(8)	1.83 (1)	O(5)–C(6)	1.20 (1)
P(1)–C(11)	1.80 (1)	N(1)–C(91)	1.12 (2)
P(1)–C(21)	1.80 (1)	C(3)–C(4)	1.46 (2)
P(2)–C(8)	1.83 (1)	C(4)–C(5)	1.30 (1)
P(2)–C(31)	1.86 (1)	C(5)–C(6)	1.46 (2)
P(2)–C(41)	1.85 (1)	C(91)–C(92)	1.53 (2)
P(3)–C(9)	1.82 (1)		
	(b) Nonbonded Distances		
Ir(1)–Ir(2)	3.4580 (7)	P(3)–P(4)	3.142 (5)
P(1)–P(2)	3.150 (4)		

[a] Numbers in parentheses are estimated standard deviations in the least significant figures.

C═O double bonds in the dimethyl acetylenedicarboxylate moiety; all are normal for such distances in organic carbonyls. Although there is a slight asymmetry in the carbonyl ligand (Figure 2), it is not large and may reflect a combination of electronic influences, due to the two differing Ir environments, and steric effects, with O(1) being forced away from the more crowded metal center (Ir(2)).

The structural parameters of the bridging alkyne group are consistent with its formulation as a dimetalated olefin. Therefore, all angles around the two olefinic carbons (C(4) and C(5)) are approximately 120° and the C(4)–C(5) distance (1.30 (1) Å) is close to that of a normal olefin.[17] The two methoxycarbonyl moieties are skewed from each other by 87.8°, and as a result one lies almost parallel to the olefinic plane while the other is almost perpendicular to it. The orientation of the latter CO_2Me group allows coordination of the acetonitrile ligand adjacent to it while the orientation of the former group seems to block the vacant coordination site on Ir(1) (see Figures 1 and 2). As a result Ir(1) appears unable to achieve an 18-electron configuration like Ir(2) by coordinating a second NCMe group. Other parameters within the DMA ligand are as expected.

The acetonitrile ligand is bound in a normal end-on fashion and is essentially linear. The N(1)–C(91) and C(91)–C(92) distances are consistent with the expected triple- and single-bond values, and the Ir(2)–N(1) distance is also normal. Surprisingly, both Ir–Cl distances are identical even though their environments differ substantially with Cl(2) being more nearly trans to a σ-bound carbon atom of high trans influence.[18-20]

The present structure quite closely resembles that of $[Rh_2(O_2CMe)(P(OMe)_3)(\mu\text{-}CO)(\mu\text{-}DMA)(DPM)_2][PF_6]$,[7] having a five- and a six-coordinate metal bridged by two DPM groups, an alkyne, and a "ketonic" carbonyl group. The six-coordinate metal

---

(17) *International Tables for X-ray Crystallography*; Kynoch: Birmingham, England, 1974; Vol. III, Table 4.2.2.

(18) Cowie, M.; Ibers, J. A. *Inorg. Chem.* **1976**, *15*, 552.

(19) Itoh, I.; Matsuda, I.; Ueda, F.; Ishii, Y.; Ibers, J. A. *J. Am. Chem. Soc.* **1977**, *99*, 2118.

(20) Cetinkaya, B.; Lappert, M. F.; McLaughlin, G. M.; Turner, K. *J. Chem. Soc., Dalton Trans.* **1974**, 1591.

Table V. Selected Angles (deg) in Compound **5**[a]

Cl(1)-Ir(1)-P(1)	97.5 (1)	C(8)-P(2)-C(41)	104.4 (5)
Cl(1)-Ir(1)-P(3)	93.4 (1)	C(31)-P(2)-C(41)	100.9 (5)
Cl(1)-Ir(1)-C(1)	114.4 (4)	Ir(1)-P(3)-C(9)	113.9 (4)
Cl(1)-Ir(1)-C(4)	157.1 (3)	Ir(1)-P(3)-C(51)	114.0 (4)
P(1)-Ir(1)-P(3)	168.9 (1)	Ir(1)-P(3)-C(61)	120.3 (5)
P(1)-Ir(1)-C(1)	88.8 (3)	C(9)-P(3)-C(51)	102.2 (6)
P(1)-Ir(1)-C(4)	84.3 (3)	C(9)-P(3)-C(61)	103.4 (6)
P(3)-Ir(1)-C(1)	88.3 (4)	C(51)-P(3)-C(61)	100.7 (6)
P(3)-Ir(1)-C(4)	84.9 (3)	Ir(2)-P(4)-C(9)	111.8 (4)
C(1)-Ir(1)-C(4)	88.5 (5)	Ir(2)-P(4)-C(71)	113.5 (4)
Cl(2)-Ir(2)-P(2)	92.8 (1)	Ir(2)-P(4)-C(81)	119.7 (4)
Cl(2)-Ir(2)-P(4)	92.6 (1)	C(9)-P(4)-C(71)	106.3 (5)
Cl(2)-Ir(2)-N(1)	82.5 (3)	C(9)-P(4)-C(81)	104.0 (6)
Cl(2)-Ir(2)-C(1)	98.5 (4)	C(71)-P(4)-C(81)	100.2 (6)
Cl(2)-Ir(2)-C(5)	173.3 (3)	C(2)-O(2)-C(3)	117 (1)
P(2)-Ir(2)-P(4)	172.4 (1)	C(6)-O(4)-C(7)	117 (1)
P(2)-Ir(2)-N(1)	93.7 (3)	Ir(2)-N(1)-C(91)	174 (1)
P(2)-Ir(2)-C(1)	87.2 (3)	Ir(1)-C(1)-Ir(2)	119.4 (6)
P(2)-Ir(2)-C(5)	87.4 (3)	Ir(1)-C(1)-O(1)	113.5 (8)
P(4)-Ir(2)-N(1)	92.2 (3)	Ir(2)-C(1)-O(1)	127.0 (9)
P(4)-Ir(2)-C(1)	86.8 (3)	O(2)-C(3)-O(3)	119 (1)
P(4)-Ir(2)-C(5)	87.8 (3)	O(2)-C(3)-C(4)	111 (1)
N(1)-Ir(2)-C(1)	178.7 (5)	O(3)-C(3)-C(4)	130 (1)
N(1)-Ir(2)-C(5)	90.9 (4)	Ir(1)-C(4)-C(3)	117.0 (9)
C(1)-Ir(2)-C(5)	88.2 (5)	Ir(1)-C(4)-C(5)	122.7 (8)
Ir(1)-P(1)-C(8)	114.3 (4)	C(3)-C(4)-C(5)	120 (1)
Ir(1)-P(1)-C(11)	113.1 (4)	Ir(2)-C(5)-C(4)	121.3 (8)
Ir(1)-P(1)-C(21)	119.0 (4)	Ir(2)-C(5)-C(6)	117.5 (8)
C(8)-P(1)-C(11)	100.8 (5)	C(4)-C(5)-C(6)	121 (1)
C(8)-P(1)-C(21)	104.8 (5)	O(4)-C(6)-O(5)	120 (1)
C(11)-P(1)-C(21)	102.7 (6)	O(4)-C(6)-C(5)	111 (1)
Ir(2)-P(2)-C(8)	112.1 (4)	O(5)-C(6)-C(5)	129 (1)
Ir(2)-P(2)-C(31)	121.2 (4)	P(1)-C(8)-P(2)	118.9 (6)
Ir(2)-P(2)-C(41)	112.9 (4)	P(3)-C(9)-P(4)	117.7 (6)
C(8)-P(2)-C(31)	103.5 (5)	N(1)-C(91)-C(92)	179 (2)

[a] Numbers in parentheses are estimated standard deviations in the least significant digits.

in this rhodium species has one bidentate acetate ligand instead of a chloro and an acetonitrile group as in our species. Nevertheless, the influence on the bridging alkyne group is similar, with the two structures having comparable orientations of the methoxycarbonyl substituents. Other parameters in the two structures are also closely comparable. It is possibly significant that the lower stretching frequency for the bridging carbonyl group in **5** (this value is 1712 cm^{-1} in the above Rh species[7]) is matched by a somewhat longer C-O distance. This is consistent with greater π back-donation from the more basic Ir centers.

Discussion of Results

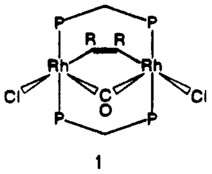

1

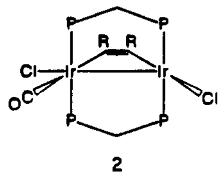

2

As noted in the Introduction, the two complexes $[M_2Cl_2(CO)(\mu\text{-DMA})(DPM)_2]$ (M = Rh (**1**), Ir (**2**)) are structurally rather different. Whereas **1** has the carbonyl ligand bridging the metals and has no metal-metal bond,[5] compound **2** has a terminal CO group with an accompanying metal—metal bond.[9] As a result, the metals in compound **1** are in identical chemical environments, with both having 16-electron configurations, whereas in **2** the metals differ, with one having 18 and the other having 16 valence electrons.

The coordinatively unsaturated end of compound **2** resembles the two metal centers in the symmetric compound $[Rh_2Cl_2(\mu\text{-}CF_3C_2CF_3)(DPM)_2]$,[21] suggesting that, as for this rhodium species, ligand addition should be possible. Extended Hückel calculations on this rhodium A-frame and related species[22,23] indicated that the LUMO in each complex was such that attack by small molecules such as CO was possible either at the endo sites opposite the bridging groups ($CF_3C_2CF_3$,[21] CO,[24] or SO_2[25]) or at the exo sites adjacent to these bridging groups. Although the calculations did not seem to favor one site of attack over the other, experimental evidence on the reactions with CO and SO_2[24,26] suggested that in these metal-metal-bonded A-frames attack was favored at the endo sites. By contrast, CO attack on the non-metal-metal-bonded A-frame $[Rh_2(CO)_2(\mu\text{-}Cl)(DPM)_2]^+$ was observed to occur at the exo site.[27]

Consistent with the above suggestions, compound **2** does react with several small molecules, including CO, NCMe, PMe_3, and $P(OMe)_3$, to give one of two types of species.[28] Reaction of **2** with CO yields the dicarbonyl species **6**, which had been previously characterized.[9] This species has two chemically inequivalent iridium centers, giving rise to a complex $^{31}P\{^1H\}$ NMR spectrum that is typical for such species and shows two terminal carbonyl bands as well as stretches due to the C=C and C=O moieties of the dimetalated olefin group (Table I). An X-ray structure determination of this species[9] showed that it had the structure given here and on the basis of the proposed structure for **2** (vide infra) suggests that CO attack occurs at the exo site. Presumably the CO group on the adjacent, six-coordinate metal center of **2** sterically inhibits CO attack at the endo site and instead favors exo attack. This product (**6**) is the expected result of ligand association at the unsaturated metal of compound **2**, giving rise to similar, although not identical, chemical environments at the two 18-electron centers.

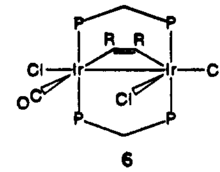

6

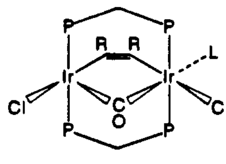

L = PMe_3 (**3**), $P(OMe)_3$ (**4**), NCMe (**5**)

The products obtained in the reactions of **2** with the ligands PMe_3, $P(OMe)_3$, and NCMe, on the other hand, differ substantially from that obtained with CO. Certainly, as judged by the structure of the NCMe adduct **5** (vide supra), ligand attack has again occurred at the exo site, and the resulting positions of the CO and Cl groups offer confirmation of the structure proposed for **2** (the other possible isomer having the CO group opposite the Ir-Ir bond and Cl opposite the alkyne seems less likely).[9] However, on the basis of the structure of **5** and on the similarities in spectral parameters between compounds **3**, **4**, and **5**, it seems that coordination of the groups PMe_3, $P(OMe)_3$, and NCMe is accompanied by movement of the terminal CO to the bridging site with concomitant Ir-Ir bond cleavage. The resulting products have the unusual "ketonic" carbonyl group[8] and have electron configurations that are reversed from those in the starting material

---

[21] Dickson, R. S.; Cowie, M. *Inorg. Chem.* **1981**, *20*, 2682.

[22] Hoffman, D. M.; Hoffmann, R. *Inorg. Chem.* **1981**, *20*, 3543.

[23] Hoffman, D. M.; Hoffmann, R.; Fisel, C. R. *J. Am. Chem. Soc.* **1982**, *104*, 3858.

[24] Cowie, M.; Dwight, S. K. *Inorg. Chem.* **1980**, *19*, 2508.

[25] Cowie, M.; Dwight, S. K. *Inorg. Chem.* **1980**, *19*, 209.

[26] Cowie, M.; Dickson, R. S.; Hames, B. W. *Organometallics* **1984**, *3*, 1879.

[27] Mague, J. T.; Sanger, A. R. *Inorg. Chem.* **1979**, *18*, 2060.

[28] The reactions with CNMe and CN-*t*-Bu were also attempted; however, these proceed quite differently, giving complex mixtures of products under a variety of stoichiometries. Presumably this chemistry is similar to that reported in ref 26.

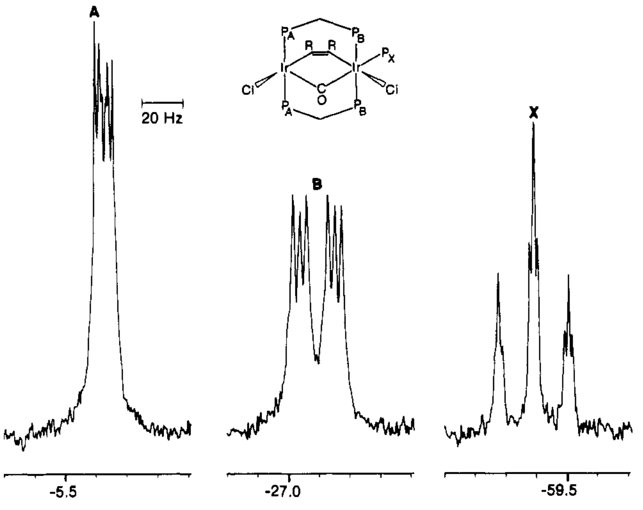

Figure 3. $^{31}P\{^1H\}$ NMR spectrum for compound **3** run at 161.98 MHz. P_A and P_B are the chemically inequivalent ends of the DPM ligands, and P_X is the PMe_3 ligand.

2; now Ir(1) has 16 electrons and Ir(2) has 18 electrons. Compounds **3**–**5** display IR stretching frequencies for the bridged carbonyl groups between 1608 and 1635 cm^{-1}. These values are even lower than those of the carbonyl groups on the bridging DMA ligands (between 1680 and 1705 cm^{-1} in these species) and are consistent with their sp^2-hybridized formulations. The bridging carbonyl stretch in ^{13}CO-labeled compound **5** (prepared from ^{13}CO-labeled **2**) was clearly identified at 1599 cm^{-1}, while the stretches of the DMA carbonyls remained essentially unchanged from those in the unenriched sample. The three compounds also display similar $^{31}P\{^1H\}$ NMR resonances for the DPM groups, having one low-field signal at ca. −3.7 ppm and a high-field signal at ca. −25.2 ppm. The $^{31}P\{^1H\}$ NMR spectrum for the PMe_3 adduct (**3**) is shown in Figure 3 and is clearly consistent with the formulation shown. The PMe_3 resonance at high field (P_X) is split into a triplet by the two adjacent and chemically equivalent P_B nuclei of the DPM group and further split into a minor triplet due to long-range coupling with the two P_A nuclei. Both the P_A and P_B resonances are complex second-order patterns, as is usually the case in DPM-bridged species,[9,26,27,29] with the P_B resonance being further split into a doublet by coupling with P_X, and P_A appearing as an unresolved multiplet due to the long-range coupling to P_X superimposed on the second-order spectrum. Selective decoupling of the P_A, P_B, and P_X nuclei in turn confirms the coupling assignments, and in particular, decoupling the P_X nucleus results in simplified resonances for both P_A and P_B in which each resembles half of that shown in Figure 3 for P_B. The $^{31}P\{^1H\}$ NMR spectrum for the $P(OMe)_3$ adduct **4** appears very similar to that of **3**, except that the $P(OMe)_3$ resonance is found at low field as is typically observed in phosphites.[30] As shown in Table I, the ^1H NMR resonances for complexes **3** and **4** are also consistent with the proposed structures.

The X-ray structure determination for compound **5** unambiguously confirms the proposed structure for this NCMe adduct, and as noted, the similarities in most spectral parameters suggest that complexes **3** and **4** have analogous structures. In addition the solution IR spectra match the solid spectra quite closely and none of the species reported show any significant conductivity in CH_2Cl_2 (the solvent of study), suggesting that the solid-state and solution structures are similar. In compound **5** the N≡C stretch of the acetonitrile group was not identified, but this is not unusual given that these stretches are often weak at best. The ^1H NMR spectrum showed three methyl resonances corresponding to the NCMe group and the two inequivalent ends of the dimethyl acetylenedicarboxylate ligand. As a related aside, we note that the structure observed for **5** and proposed for **3** and **4** is analogous to the expected product in the reaction of **1** with small molecules. Although it was suggested that the formation of such adducts should be possible,[22] this was not unambiguously confirmed experimentally for the rhodium species.

An understanding of why the structure of the CO adduct (**6**) differs from those of the PMe_3 (**3**), $P(OMe)_3$ (**4**), and NCMe (**5**) adducts, can be obtained through a consideration of the nature of the bonding involving these four ligands. Clearly what sets CO apart from the others is its superb π acidity; although the others have some π-acid character, this is much less than that of CO, and the other ligands are probably better σ donors.[31,32] A consideration of the proposed structure for compound **2** shows that one metal differs from the other in having a coordinated CO ligand. In spite of the fact that this metal is coordinatively saturated, the better π-accepting capability of CO compared to its σ-donor ability leads us to suggest that it is the coordinatively unsaturated metal that is more electron rich. Coordination of another carbonyl ligand, at the unsaturated metal, yielding the expected adduct **6**, serves to remove the excess electron density. However, coordination of a ligand that is a good σ-donor but a poor π-acceptor (e.g. PMe_3, $P(OMe)_3$, NCMe) at the electron-rich metal causes additional electron density buildup that can only be alleviated by movement of the terminal carbonyl group into the bridging position, where it can function to remove electron density from both metals. Since in the proposed initial adduct of compound **2** (which should be analogous to **6**) both metals are coordinatively saturated, CO migration can only occur with accompanying Ir–Ir bond cleavage. The very low carbonyl stretches in these compounds bear witness to the efficiency of the resulting ketonic carbonyl groups at removing the excess electron density.

We have observed in this chemistry an interesting example involving the transmission of electronic influences; the electron-density buildup at one metal results in the transfer of a carbonyl group from the *other* metal to the bridging position. Presumably it is the stability gained by this redistribution of electron density that favors this unusual ketonic carbonyl binding mode in these compounds. This suggests that it may be possible to induce the transformation of a terminal to a bridging carbonyl group with accompanying Ir–Ir bond cleavage in species analogous to **2** by utilizing more basic ancillary ligands, such as $Me_2PCH_2PMe_2$, instead of DPM. Such studies are currently under way.

Acknowledgment. We thank the University of Alberta and the Natural Sciences and Engineering Research Council of Canada for financial support of this research, The University of Alberta for funding the visit by G.V., the NSERC for a scholarship to B.R.S. and partial funding of the diffractometer through a grant to M.C., and Johnson Matthey for a generous loan of iridium trichloride. We also thank Glen Bigam and Tom Brisbane for assistance with the NMR experiments and Dr. Stephen J. Sherlock for technical assistance.

Registry No. **2**, 92270-18-3; **3**, 102307-83-5; **4**, 102307-84-6; **5**, 102307-85-7; **6**, 92270-14-9.

Supplementary Material Available: Listings of bond lengths and angles within the phenyl groups, least-squares planes, anisotropic thermal parameters, and idealized hydrogen parameters (5 pages). Ordering information is given on any current masthead page.

---

(29) Gibson, J. A. E.; Cowie, M. *Organometallics* **1984**, *3*, 722.

(30) Mark, V.; Dungan, C. H.; Crutchfield, M. M.; van Wazer, J. R. *Top. Phosphorus Chem.* **1967**, *5*, 227.

(31) Graham, W. A. G. *Inorg. Chem.* **1968**, *7*, 315.

(32) Huheey, J. E. *Inorganic Chemistry: Principles of Structure and Reactivity*, 3rd ed.; Harper and Row: New York, 1983; p 436.